Chinese Chemical Letters 36 (2025) 109956

Contents lists available at ScienceDirect

Chinese Chemical Letters

journal homepage: www.elsevier.com/locate/cclet

Discovery of amentoflavone as a natural PDE4 inhibitor with anti-fibrotic effects

Zhexin Chen[a,1], Yuqing Shi[a,c,1], Fang Zhong[a], Kai Zhang[a,c], Furong Zhang[a,c], Shenghong Xie[a], Zhongbin Cheng[a], Qian Zhou[a,*], Yi-You Huang[a,*], Hai-Bin Luo[a,b,*]

[a] Key Laboratory of Tropical Biological Resources of Ministry of Education and Hainan Engineering Research Center for Drug Screening and Evaluation, School of Pharmaceutical Sciences, Hainan University, Haikou 570228, China
[b] Song Li' Academician Workstation of Hainan University (School of Pharmaceutical Sciences), Sanya 572000, China
[c] School of Life and Health Sciences, Hainan University, Haikou 570228, China

ARTICLE INFO

Article history:
Received 15 March 2024
Revised 26 April 2024
Accepted 30 April 2024
Available online 1 May 2024

Keywords:
Phosphodiesterase-4
Inhibitor
Amentoflavone
Crystal structure
IPF

ABSTRACT

Idiopathic pulmonary fibrosis (IPF) is a progressive lung disease with high mortality rate but effective therapeutics are still lacking. Phosphodiesterase-4 (PDE4) inhibitors were reported to be promising anti-IPF agents. Herein, series of biflavonoids isolated from *Selaginella uncinate* were found to be PDE4 inhibitors and the most active amentoflavone gave a half maximal inhibitory concentration (IC_{50}) of 12 nmol/L, which was further validated by isothermal titration calorimetry with K_d of 23 nmol/L. Besides, co-crystal structure of PDE4-amentoflavone was determined and gave a different binding pattern from roflumilast with multiple H-bonds between it and key residues such as Asn321/Thr333/Gln369/Gly371. So far, this was the first reported co-crystal structure of amentoflavone with its potential binding target in despite of the extensive investigations of this common natural biflavonoid. Furthermore, amentoflavone exhibited remarkable anti-IPF effects *in vivo* and *in vitro*, suggesting it as a novel anti-fibrotic agent by targeting PDE4.

Idiopathic pulmonary fibrosis (IPF) is a chronic and progressive lung disease characterized by collagen deposition, alveolar inflammation, fibroblast proliferation and the destruction of lung tissue structures, which leads to decreased lung compliance, and ultimately respiratory failure and death [1,2]. The incidence rate of IPF is rising in regard of the prevalence of corona virus disease 2019 (COVID-19) fibrotic diseases [3]. However, up to date, only two drugs (pirfenidone and nintedanib) are available for the treatment of IPF and both can slow down but not halt the disease progression [4]. As a result, the median survival time of the IPF patients after diagnosis is only 2–4 years [5]. Therefore, IPF is a mortal disease and novel therapeutic drugs are still urgently needed.

Phosphodiesterase-4 (PDE4) is a promising drug target for treatment of IPF. It is reported that inhibition of PDE4 could increase intracellular levels of cyclic adenosine monophosphate (cAMP), affect the inflammatory responses and fibrotic processes, including reducing the release of pro-inflammatory mediators and recruitment of inflammatory cells [6]. The selective PDE4 inhibitor roflumilast has proven to have *in vivo* and *in vitro* anti-fibrotic effects in IPF models [7]. Besides, the newly reported PDE4 inhibitor BI 1015550 showed to effectively stabilize lung function of IPF patients in clinical trials, which further validated the feasibility of PDE4 as a potential target of IPF [8]. However, the clinical use of PDE4 inhibitors are usually limited by side effects such as emesis and nausea. These drawbacks might be addressed to the common catechol moieties that they shared in the structures and the exploitation of structurally diverse PDE4 inhibitors with enhanced efficacy and reduced side effects is still compelling. Recently, series of PDE4 inhibitors derived from the natural α-mangostin were reported to have greater safety profiles compared to the common rolipram or roflumilast [9,10], suggesting natural products could be an important source for developing novel PDE4 inhibitors.

In our continuous search for natural PDE4 inhibitors from medicinal plants, a fraction of the ethanol extract of *Selaginella uncinata* [11] showed a remarkable inhibitory rate of 91.2% at 0.1 μg/mL. Subsequent chemical investigation led to the isolation of several biflavonoids (Fig. 1) with potent PDE4 inhibitory potency and the principal constituent was found to be the most active compound amentoflavone. Amentoflavone is a well-known bi-

* Corresponding authors.
E-mail addresses: zhouqian@hainanu.edu.cn (Q. Zhou), hyyou@hainanu.edu.cn (Y.-Y. Huang), hbluo@hainanu.edu.cn (H.-B. Luo).
[1] These authors contributed equally to this work.

https://doi.org/10.1016/j.cclet.2024.109956
1001-8417/

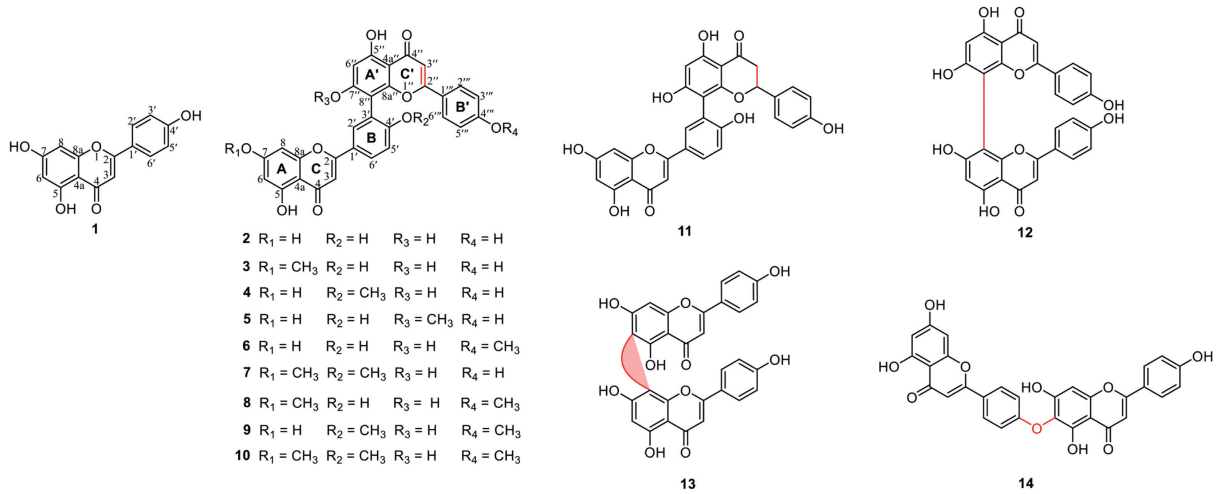

Fig. 1. The chemical structures of apigenin (**1**) and biflavonoids (**2**–**14**).

flavonoid occurring in many plants and has been extensively investigated with multifunctional biological activities such as anti-inflammatory, anti-microorganism, anti-cancer and metabolism regulation [12]. Although amentoflavone might exert therapeutic benefits by targeting various proteins/enzymes with moderate activities [13], the direct binding evidences of amentoflavone were still lacking and no co-crystal structures of amentoflavone with possible targets were available in the RCSB PDB database. Herein, details of the isolation/modification, structural elucidation, inhibiting/binding profiles against PDE4, and anti-fibrotic effects of amentoflavone are described.

The air-dried powder of the aerial part of *Selaginella uncinata* (5 kg) was extracted with 95% ethanol (3 × 10 L) at room temperature (rt) to give 290 g of crude extract. The extract was suspended in H_2O (1 L) and then sequentially partitioned with petroleum mether (PE, 3 × 1 L), ethyl acetate (EtOAc, 3 × 1 L), and *n*-butanol (*n*-BuOH, 3 × 1 L). The solutions were concentrated in vacuum to obtain the corresponding fractions: petroleum ether extract (62.14 g), ethyl acetate extract (43.48 g) and *n*-butanol extract (10.33 g). The EtOAc extract was subjected to MCI gel column chromatography (CC) eluted with a MeOH/H_2O gradient (1:9 → 10:0) to afford four fractions (Fr. A–D). Fr. C was separated by octadecylsilyl silica gel (ODS) to yield two fractions Fr. C1 and C2. The former was purified by HPLC with MeOH/H_2O (50:50, 0.1% CH_3COOH, 6 mL/min) to yield compound **2** (200 mg, t_R 13 min and 98.78% purity), while the latter was fractionated using ODS with a gradient of MeOH/H_2O (3:7 → 10:0) to give fifteen fractions Fr. C2a-Fr. C2o. Compound **13** (3.6 mg, t_R 27 min) was obtained by purification of Fr. C2e on HPLC using a mobile phase of CH_3CN/H_2O (30:70, 2 mL/min). Fr. C2g (180 mg) was purified by high performance liquid chromatography (HPLC) with CH_3CN/H_2O (40:60, 0.1% CH_3COOH) to afford compounds **1** (2.3 mg, t_R 16 min) and **12** (4.5 mg, t_R 18 min). Fr. C2h (110 mg) was purified by HPLC using the mobile phase MeOH/H_2O (60:40, 0.1% CH_3COOH, 2 mL/min) to yield compound **11** (5.2 mg, t_R 26 min). Fraction Fr. D (696 mg) was eluted with MeOH/H_2O (5:5→10:0) on an ODS to afford 14 fractions (Fr. D1-D14). Fr. D4 (21 mg) was further separated by HPLC (CH_3CN/H_2O = 45:55, 2 mL/min) to give compound **4** (5.2 mg, t_R 21 min). Fr. D5 (47 mg) was further purified by HPLC (CH_3CN/H_2O, 45:55, 2 mL/min) to give compound **6** (5.5 mg, t_R 29 min) and **14** (3.9 mg, t_R 34 min). Fr. D6 (61 mg) was purified by HPLC (CH_3CN/H_2O, 50:50, 2 mL/min) to give compounds **7** (3.8 mg, t_R 30 min) and **9** (8.6 mg, t_R 35 min).

The methyl substitution modification on the principal compound **2** was performed to enhance the structural diversity. K_2CO_3 (41 mg) was added to the solution of **2** (11 mg) in CH_3CN (0.3 mL) and the mixture was stirred at rt for 10 min followed by the addition of 1.3 mL of CH_3I in ice bath. The reaction was then transferred to an oil bath maintained at 65 °C and stirred overnight. The completion of the reaction was monitored by thin-layer chromatography (TLC). The reaction mixture was diluted with 10 mL of water and then extracted with EtOAc for three times to obtain an EtOAc extract (14 mg). However, only one pure compound **8** (3.1 mg) was yielded by HPLC using CH_3CN/H_2O (70:30, 3 mL/min).

The isolated compounds were identical to the structures of apigenin (**1**) [14], amentoflavone (**2**) [15], bilobetin (**4**) [15], podocarpusflavone A (**6**) [16], ginkgetin (**7**) [15], putraflavone (**8**) [17], isoginkgetin (**9**) [15], 2″,3″-dihydroamentiflavone (**11**) [18], cupressuflavone (**12**) [19], agathisflaxone (**13**) [20], and hinokiflavone (**14**) [15], based on comparisons of their nuclear magnetic resonance (NMR) data with those reported in the literature (Supporting information). In order to explore the structure-activity relationship as much as possible, other three compounds with different methyl substitutions, including sequoiaflavone (**3**), sotetsuflavone (**5**) and sciadopitysin (**10**), were purchased from Topscience for subsequent PDE4 activity screening.

The aforementioned compounds (**1**–**14**) were subject to the PDE4 activity assays using the ^{3}H-cAMP as substrate by a PerkinElmer MicroBeta liquid scintillation counter. The protocols were similar to those in previous literatures [9,10], and rolipram served as the positive control with a half maximal inhibitory concentration (IC_{50}) of 590 nmol/L which was comparable to the literature value. As a result, all the tested biflavonoids inhibited PDE4 with IC_{50} ranging from 12 nmol/L to 920 nmol/L (Table 1), which were more potent than the monomer flavone apigenin (**1**, 1980 nmol/L). Among them, amentoflavone (**2**) was the most po-

Table 1
IC_{50} values of the biflavonoids against PDE4D.

Compound	IC_{50} (nmol/L)	Compound	IC_{50} (nmol/L)
1	1980 ± 420	**8**	33 ± 5
2	12 ± 1	**9**	84 ± 8
3	20 ± 2	**10**	100 ± 17
4	272 ± 2	**11**	188 ± 6
5	107 ± 7	**12**	920 ± 169
6	31 ± 9	**13**	704 ± 61
7	191 ± 17	**14**	773 ± 102
Rolipram[a]	590 ± 50		

[a] Positive control.

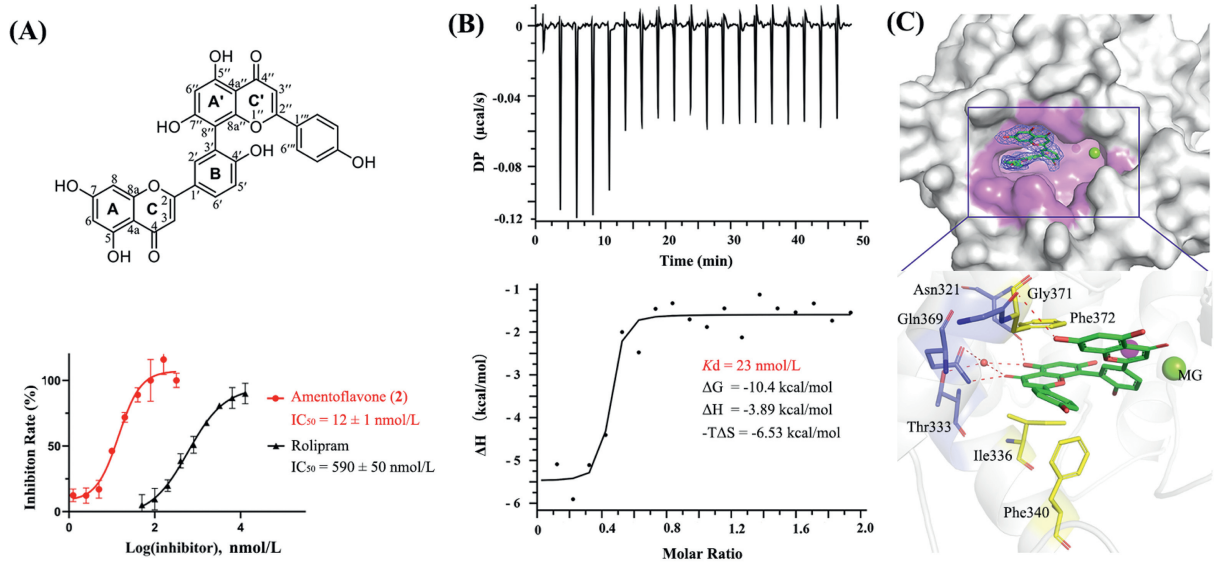

Fig. 2. The inhibitory/binding profiles of amentoflavone (**2**) with PDE4. (A) Inhibitory curve of **2** against PDE4 in enzymatic assay. IC_{50} data were calculated by the nonlinear regression method and presented as mean ± standard deviation (SD) ($n = 3$). (B) The binding affinity of **2** with PDE4 determined by ITC. (C) The co-crystal structure of PDE4–**2** (PDB ID: 8YLC). The 2Fo–Fc electron density is contoured in dark blue at 1.0 σ and H-bonds are presented in red dotted lines.

tent one with an IC_{50} of 12 nmol/L that was quite rare in natural PDE4 inhibitors, and the dose–response curve was presented in Fig. 2A. Minor structural modifications of compound **2**, such as the methyl substitution of hydroxyl groups at 7, 4′, 7′ and 4″ sites to compounds **3**–**10**, and dihydrogen reduction of double bond Δ2″ ring in **11**, would reduce the inhibitory potency at different degrees. Varied C-C or C-O-C connecting bond positions in flavonoid-flavonoid dimers such as 8–8″, 8–6″ and 6–4‴ yielded biflavonoids **12**–**14,** which showed greatly reduced PDE4 inhibitory potencies compared to **2**. Besides, we had tested the selectivity profiles of **2** against other PDE isoforms. The inhibitory IC_{50} values of **2** against PDE1B2 (10–487), PDE5A1 (535–860), PDE8A1 (480–828) and PDE9A2 (181–506) were tested to be 24, 154, 2890 and 185 nmol/L, respectively, which suggested Amentoflavone as a pan-PDE inhibitor.

The thermodynamic property of amentoflavone (**2**) binding to the catalytic domain of PDE4 in solution was also determined by isothermal titration calorimetry (ITC) measurement. As shown in Fig. 2B, the representative result and fitting curve indicated that the binding of **2** to PDE4 was driven by both enthalpy (ΔH) and entropy term ($-T\Delta S$) corresponding to some beneficial specific interactions and chaos changes, respectively. The tested binding constant K_d (23 nmol/L) was consistent with the IC_{50} value of 12 nmol/L in the enzymatic test, which further validated the high binding affinity of **2** to PDE4.

Besides, the co-crystal structure of amentoflavone (**2**) with PDE4 was successfully determined using similar protocol as previously described [21]. As shown in Fig. 2C, the electron density in 2Fo–Fc unambiguously revealed that **2** was bound in the catalytic pocket of PDE4. The highly conjugated 2-phenylchromone moiety of **2**, composed of A′/C′/B′, was sandwiched by the hydrophobic clamp consisting of Phe372 and Ile336/Phe340, and the oxygen atom of 4″ site formed a H-bond with residue Gln369. The stacking interaction with clamp and H-bonds with Gln369 were two characteristic binding modes in many PDE inhibitors. **2** is a polyphenolic compound and had multiple hydroxyl/carbonyl groups facilitated the formation of a strong H-bonds network with PDE4, including the direct or water-medicating H-bonds between the oxygen atoms of 4″/5″ sites and residues Asn321/Thr333/Gln369, and H-bond between the hydroxyl group of 7 site and residue Gly371, which were very different from the binding patterns of roflumilast. Therefore, the strong specific H-bonds network and hydrophobic interactions made contributions to the beneficial ΔH and $-T\Delta S$ resulting in the high binding affinity of **2** with PDE4. The atomic coordinate and structure factor of amentoflavone with PDE4D had been deposited into the RCSB Protein Data Bank with accession number 8YLC. Authors will release the atomic coordinate and experimental data upon article publication.

The rat liver microsome test showed that the $T_{1/2}$ value of **2** was 154 min suggesting a reasonable metabolic stability for the pharmacodynamic researches. As PDE4 is a promising drug target for treatment of IPF, the anti-fibrotic effects of PDE4 inhibitor amentoflavone (**2**) were primarily assessed *in vitro* in transforming growth factor-β (TGF-β) induced NIH-3T3 and A549 cell models, which could simulate the fibroblast-myofibroblast transition (FMT) and epithelial-mesenchymal transition (EMT) processes during the pathogenesis of IPF, respectively. As shown in Fig. 3, treatments with compound **2** dose dependently reversed TGF-β1 induced increases protein level of representative fibrosis markers including collagen I (COL1A1), and α-smooth muscle actin (α-SMA). Meanwhile, **2** could inhibit the progress of EMT as indicated by decreased levels of the N-cadherin and vimentin in dose dependent manner.

Furthermore, the bleomycin (BLM)-induced IPF mouse model was used to evaluate the *in vivo* anti-fibrotic effect of amentoflavone (**2**) as described in Fig. 4. All animal care and experimental programs were in line with the “Guide of Laboratory Animals” (National Institutes of Health Publication, revised 1996, No. 86-23, Bethesda, MD) and approved by the Institutional Ethical Committee for Animal Research of Hainan University (HPI-ACUC2023069). Mice treated with BLM suffered increased lung organ coefficient from pulmonary edema or inflammation, and had declined pulmonary functions regarding of those parameters such as resistance, inspiratory capacity, forced vital capacity, lung compliance (Cchord) and vital capacity, which indicated the IPF model was successfully established. As the bioavailabilities of mentoflavone (**2**) by oral administration (p.o.) and intraperitoneal injection (i.p.) were reported to be 0.04% and 77.4%, respectively [22], the i.p. administration of **2** was preferred in this research. After 21 consecutive days treatments of the marketed drug pirfenidone (PFD, 300 mg/kg, p.o.) and compound **2** (10 mg/kg, i.p.), the IPF symptoms of mice were alleviated that the lung organ

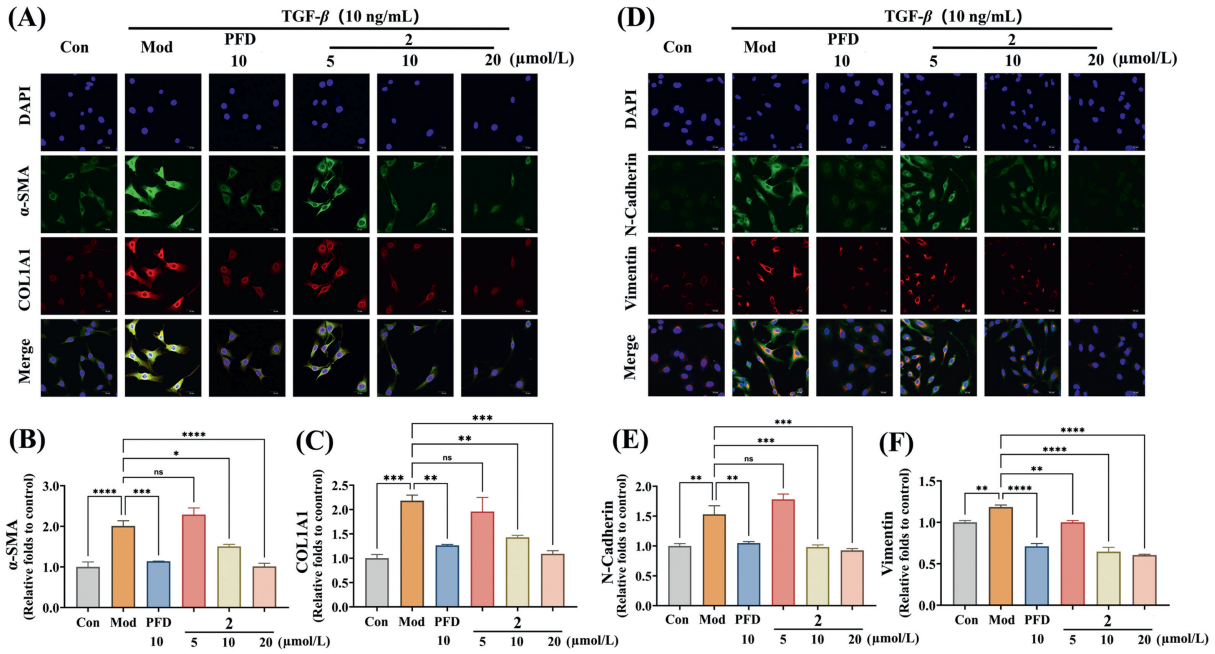

Fig. 3. The *in vitro* anti-IPF effects of **2** in TGF-β induced NIH-3T3 and A549 cell models. Pirfenidone (PFD) served as a positive control and the concentration in cell model were 10 μmol/L. (A–C) Immunofluorescence analysis of α-SMA and COL1A1 in TGF-β induced NIH-3T3 cell model. (D–F) Immunofluorescence analysis of N-cadherin and vimentin in TGF-β induced A549 cell model. Scale bar: 20 μm. DAPI, 4′,6-diamidino-2-phenylindole; ns, no significance. $^{*}P<0.05$, $^{**}P<0.01$, $^{***}P<0.001$, $^{****}P<0.0001$, compared with TGF-β-treated cells. Data are presented as mean ± standard error of the mean (SEM) ($n=3$).

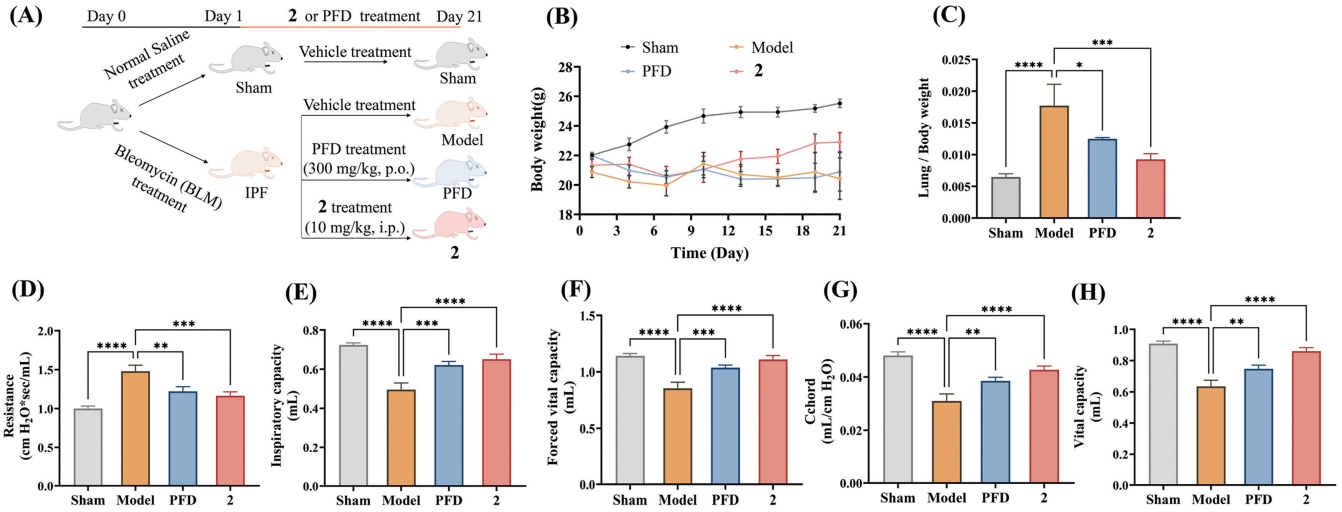

Fig. 4. The *in vivo* anti-IPF effect of **2** in BLM-induced mouse model. (A) Schematic diagram of animal study and compounds treatment. (B) The body weight of mice. (C) The ratio of lung to body weight. (D–H) The pulmonary functions of resistance, inspiratory capacity, forced vital capacity, Cchord and vital capacity. $^{*}P<0.05$, $^{**}P<0.01$, $^{***}P<0.001$, $^{****}P<0.0001$, compared with BLM-treated model mice. Data are presented as mean ± SEM ($n=8$–12 mice per group).

coefficients were obviously decreased and the damaged pulmonary functions were remarkably restored.

Further Western blot results of lung tissues (Figs. 5A–H) shown that **2** could effectively decrease the expression levels of several hallmark markers such as fibronectin 1 (FN1), COL1A1, α-SMA, N-cadherin, E-cadherin and vimentin, suggesting that the IPF therapeutic effects of **2** were arisen from inhibiting pathological processes both of EMT and FMT, which were consistent with the *in vitro* results. The subsequent hematoxylin and eosin (H&E) staining shown that **2** could effectively attenuated the lung damaged such as disordered alveoli, ruptured alveolar walls and apparent inflammatory cell infiltration, and Masson staining also figured that **2** could significantly reduce the depositions of Collagen and fibers (Fig. 5I). Determination of hydroxyproline in lung tissue also confirmed that collagen deposition was ameliorated by **2**-treatment (Fig. 5J). Therefore, amentoflavone (**2**) exhibited remarkable antifibrotic effects *in vitro* and *in vivo*.

Biflavonoids are polyphenolic compounds and widely distributed in plants, some of which have been used as traditional folk medicines for even thousands of years [23]. A majority of studies have shown that biflavonoids had privileged effectiveness of dimeric forms over the monomeric forms. As one of the well-known biflavonoids, amentoflavone (**2**) has a C3′-C8″ connecting bond and owns various important bioactivities that could be

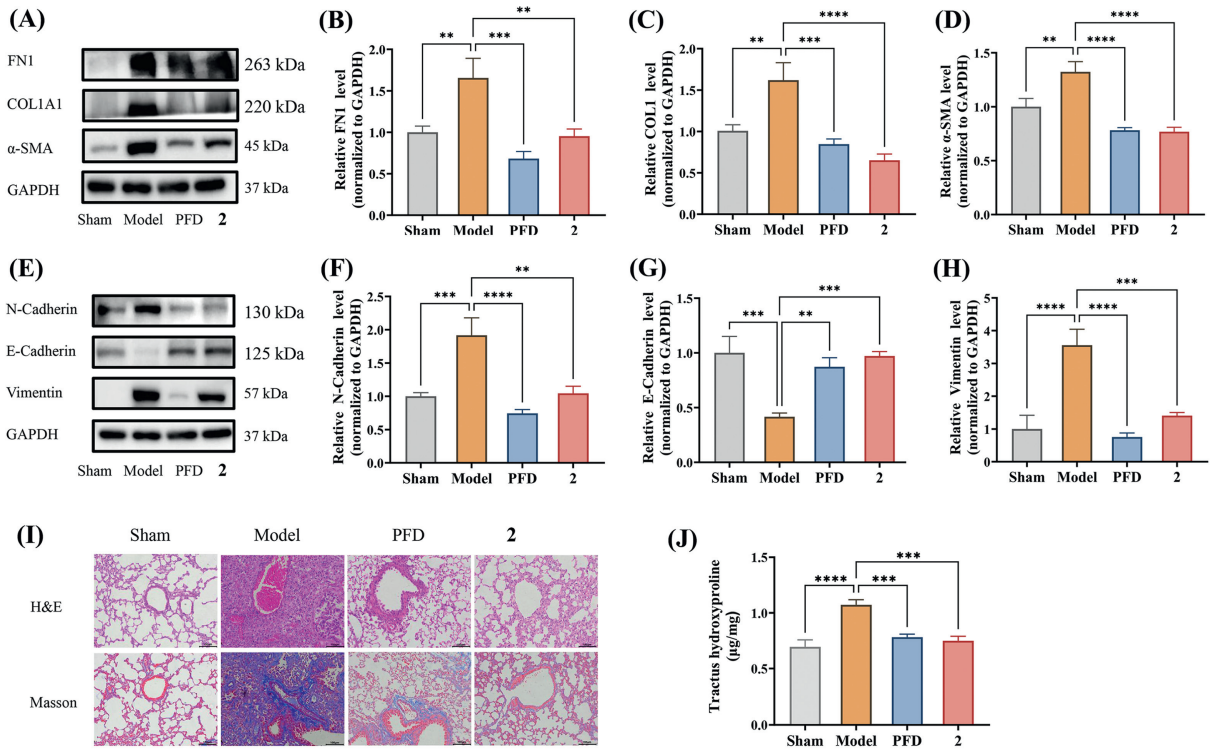

Fig. 5. Compound **2** could effectively decrease the expression levels of several hallmark markers in IPF mice. (A–D) Quantification of the protein levels of FN1, COL1A1, and α-SMA. (E–H) Quantification of the protein levels of N-cadherin, E-cadherin and vimentin. (I) Representative images of H&E staining and Masson staining. Scale bar: 100 μm. (J) The concentration of tractus hydroxyproline of lung tissues. $^{*}P < 0.05$, $^{**}P < 0.01$, $^{***}P < 0.001$, $^{****}P < 0.0001$, compared with BLM-treated model mice. GAPDH, glyceraldehyde-3-phosphate dehydrogenase. Data are presented as mean ± SEM ($n = 6$).

beneficial for treating diseases. With the development of modern pharmacology, the molecular mechanisms underlying the activities of amentoflavone were explored. For example, amentoflavone was reported to affect neutrophil function through inhibiting β-glucuronidase and also had a potential anti-inflammatory activity through the inhibition of cyclooxygenase. However, the reported binding affinities of amentoflavone with possible targets were just moderate and the direct binding evidences were still lacking. In the present work, amentoflavone was proven to be a potent PDE4 inhibitor with remarkable anti-fibrotic effects by a multidisciplinary research (natural isolation, medicinal chemistry, structural biology and pharmacology assessments), which provided crucial evidences to furtherly exploit the therapeutic potential of this biflavonoid molecule against emerging diseases.

Declaration of competing interest

The authors declare that they have no known competing financial interests or personal relationships that could have appeared to influence the work reported in this paper.

CRediT authorship contribution statement

Zhexin Chen: Methodology, Investigation, Data curation. **Yuqing Shi:** Methodology, Investigation. **Fang Zhong:** Validation, Methodology, Investigation. **Kai Zhang:** Visualization, Validation, Methodology, Investigation. **Furong Zhang:** Methodology, Investigation, Data curation. **Shenghong Xie:** Validation, Methodology, Investigation, Data curation. **Zhongbin Cheng:** Writing – review & editing, Writing – original draft, Validation, Methodology. **Qian Zhou:** Writing – review & editing, Writing – original draft, Visualization, Validation, Supervision. **Yi-You Huang:** Writing – review & editing, Writing – original draft, Visualization, Validation, Supervision, Project administration. **Hai-Bin Luo:** Supervision.

Acknowledgments

This work was supported by the Natural Science Foundation of China (Nos. 22277019, 22307031, 22077143, 22377023), Fundamental Research Funds for Hainan University (Nos. KYQD(ZR)-21031, KYQD(ZR)-21108, KYQD(ZR)-23003, XTCX2022JKA01), Science Foundation of Hainan Province (Nos. KJRC2023B10, 822MS051, 824YXQN420, 324MS018).

Supplementary materials

Supplementary material associated with this article can be found, in the online version, at doi:10.1016/j.cclet.2024.109956.

References

[1] L. Richeldi, H.R. Collard, M.G. Jones, Lancet 389 (2017) 1941–1952.
[2] T. Zhang, C. Sun, S. Yang, et al., Chin. Chem. Lett. 35 (2024) 109248.
[3] F. Patrucco, P. Solidoro, F. Gavelli, et al., Microorganisms 11 (2023) 895.
[4] T. Karampitsakos, B.M. Juan-Guardela, A. Tzouvelekis, et al., EBioMedicine 95 (2023) 104766.
[5] B. Ley, H.R. Collard, T.E. King, Am. J. Respir. Crit. Care Med. 183 (2011) 431–440.
[6] L. Richeldi, A. Azuma, V. Cottin, et al., New Engl. J. Med. 386 (2022) 2178–2187.
[7] J. Cortijo, A. Iranzo, X. Milara, et al., Br. J. Pharmacol. 156 (2009) 534–544.
[8] G. Sgalla, J. Simonetti, S. Cortese, et al., Expert Opin. Inv. Drug 32 (2023) 17–23.
[9] Y.Y. Huang, J.H. Deng, Y.J. Tian, et al., J. Med. Chem. 64 (2021) 13736–13751.
[10] J. Liang, Y.Y. Huang, Q. Zhou, et al., J. Med. Chem. 63 (2020) 3370–3380.
[11] R. Liu, H. Zou, P. Xu, et al., Chin. Chem. Lett. 28 (2017) 1465–1468.
[12] S. Yu, H. Yan, L. Zhang, et al., Molecules 22 (2017) 299.
[13] X.F. Xiong, N. Tang, X.D. Lai, et al., Front. Pharmacol. 12 (2021) 768708.

[14] J.W. Yang, Z.Y. Gu, J. Zhao, et al., Lishizhen Med. Mater. Med. Res. 22 (2011) 375–376.
[15] Y. Cao, Y.P. Wu, X.Z. Weng, et al., Nat. Prod. Res. Dev. 24 (2012) 150–154.
[16] A. Coqueiro, L.O. Regasini, S.C.G. Skrzek, et al., Molecules 18 (2013) 2376–2385.
[17] A.I. Suarez, B. Diaz M, F. Delle Monache, et al., Fitoterapia 74 (2003) 473–475.
[18] G. Skopp, G. Schwenker, Z. Naturforsch. B 41 (1986) 1479–1482.
[19] H. Li, Y. Luo, Z. He, et al., Chin. J. Appl. Environ. Biol. 13 (2007) 188–191.
[20] C. Mohan, I. Mohammed, W. Hildebert, et al., Phytochemistry (1977) 1273.
[21] Y. Huang, X. Liu, D. Wu, et al., Biochem. Pharmacol. 130 (2017) 51–59.
[22] S. Liao, Q. Ren, C. Yang, et al., J. Agric. Food Chem. 63 (2015) 1957–1966.
[23] J. Xu, X. Liu, K. Chen, Chin. Chem. Lett. 20 (2009) 939–941.